# Local nonequilibrium effect on undercooling in rapid solidification of alloys

Peter Galenko
*Institute of Mathematical Simulation, Udmurt State University, 71 Krasnogeroyskaya Street, Izhevsk 426034, Russian Federation*

Sergei Sobolev
*Institute of Chemical Physics, Russian Academy of Sciences, Chernogolovka 142432, Moscow Region, Russian Federation*
(Received 12 February 1996; revised manuscript received 31 July 1996)

A local nonequilibrium approach to rapid solidification of undercooled alloys is presented. Taking into account the finite speed of mass signals, a steady-state solution to the nonisothermal rapid solidification problem has been obtained. We have found that, if the solidification front moves at a velocity $V$ equal to or higher than the diffusive speed $V_D^L$ in the liquid, a partitionless thermal-controlled situation takes place. The solidification mechanism changes at $V=V_D^L$ and the constitutional undercooling is lacking ahead of the solidification front. Some comparisons with the known experimental and theoretical results are discussed. [S1063-651X(96)03312-0]

PACS number(s): 61.25.Mv

## I. INTRODUCTION

Considerable study has been given recently to the processes of rapid solidification, which leads to a wide spectrum of applications for production of novel materials with the advent of new sophisticated technologies such as laser and electron beam treatment of surfaces, quenching from the liquid state, and the levitation technique [1,2]. The most important practical results of rapid solidification are the formation of homogeneous solid solutions and morphological transitions in growth forms of crystals [1–4].

It is well known that rapid solidification and recrystallization occur under conditions that are far from local equilibrium [1–7]. However, as a rule, existing theoretical treatments take into account only the deviation from chemical equilibrium at the interface introducing the velocity dependent partition coefficient $k(V)$, where $V$ is the velocity of the solidification front motion [10–12]. All aspects of the models assume the local equilibrium in the bulk phases and rely on classical irreversible thermodynamics by Onsager and Prigogine. Such a modeling is only valid for a relatively low interface velocity $V \ll V_D^L$, where $V_D^L$ is the diffusive speed in the liquid, i.e., the maximum speed of propagation of the concentrational perturbations. In this case, classical thermodynamics and the transport theory give reliable results for most situations encountered in practice [1].

Solidification of undercooled melts can be so fast that the interface velocity $V$ is of the order of or even greater than the diffusive speed $V_D^i$ in the bulk liquid ($i=L$) or solid ($i=S$) [1–4,7]. In these cases there is no local equilibrium in the bulk phases and the solute flux cannot be described by the classical mass transport theory. Thus one should take into account the deviations from local equilibrium in phases which affect both the solute diffusion field and the interface kinetics. Our theoretical treatments [13–17] have shown that in rapid solidification the diffusion field in alloys (and in some special cases the thermal field in pure substances) is far from local equilibrium. In these situations the concentration (temperature) and its flux differ significantly from those predicted by the classical local equilibrium theory.

The main purpose of the present article is to obtain the undercoolings at the solidification front and in the liquid phase under local nonequilibrium conditions. The article is organized as follows. In Sec. II we consider the general model which takes into account the deviation from the local equilibrium of the diffusion field inside the phases and at the solidification front. This model incorporates the diffusive speed $V_D^i$ as the most decisive parameter governing the solute concentration field in the bulk phases. In Sec. III we consider an important case of steady-state regime of solidification, and in Sec. IV we accentuate the undercooling in the liquid phase ahead of the solidification front. Our approach is applied to the case of flat liquid-solid interface motion and we perform an analysis of the undercooling influence on the transition from diffusion-limited growth to the thermal and kinetic regimes of rapid solidification. In Sec. V, on the basis of our model we give the numerical estimates of undercoolings and solute partitioning for Ag-Cu and Si-As dilute alloys. A summary is given in Sec. VI.

## II. THE MODEL

The new approach to local nonequilibrium heat-mass transfer is nowadays generally referred to as extended irreversible thermodynamics by Jou, Casas-Vazquez, and Lebon [18] and is the subject of an increasing interest. There are some other methods which also do not adopt the local equilibrium assumption (see, for example, [13,14,19], and references therein). These theories lead to Fourier's and Fick's generalized laws by including relaxation effects, which convert the ordinary constitutive equations for the heat and mass fluxes into evolution equations for these quantities.

Let us consider the nonisothermal movement of the liquid-solid interface in a diluted chemically inert binary alloy. Using the relaxational approach [13,18] to the problem of local nonequilibrium diffusion mass transport during solidification [4,15,17,20], we may write Fick's generalized law as

 

$$\mathbf{J}_i+\tau_D^i\frac{\partial \mathbf{J}_i}{\partial t}+D_i\nabla C_i=0. \tag{2.1}$$

Here index $i$ is relative to the liquid phase ($i=L$) or the solid one ($i=S$); $C_i$ is the mass concentration of the dissolved component in a binary diluted alloy; $\mathbf{J}_i$ is the vector of the diffusion flux of the dissolved component; $\tau_D^i$ is the time of diffusional relaxation of the collective of atoms (molecules, particles) to their equilibrium state in a local volume of alloy; $D_i$ is the diffusion coefficient.

Equation (2.1) can be treated as the simplest generalization of the classical Fick law for mass transport in both phases, which takes into account the relaxation to local equilibrium of the mass flux. As it follows from Eq. (2.1), the concentration gradient $\nabla C_i$ at a point of alloy defines a mass flux not at time $t$ as in the local-equilibrium approximation but with a delay equal to the relaxation time $\tau_D^i$.

The mass transfer in both phases is governed by the balance law

$$\frac{\partial C_i}{\partial t}+\nabla\cdot\mathbf{J}_i=0. \tag{2.2}$$

In contrast with Fick's law, which leads to the diffusion equation of parabolic type, Eqs. (2.1) and (2.2) give rise to the hyperbolic equation for the solute concentration [13–20]

$$\frac{\partial C_i}{\partial t}+\tau_D^i\frac{\partial^2 C_i}{\partial t^2}=\nabla\cdot(D_i\nabla C_i). \tag{2.3}$$

Equation (2.3) is the simplest mathematical model combining the diffusive (dissipative) mode and the propagative (wave) mode of mass transport under local nonequilibrium conditions. This equation implies a finite speed $V_D^i=(D_i/\tau_D^i)^{1/2}$ of concentrational perturbations. We can also consider the speed $V_D^i$ as a maximum speed at which the diffusional perturbations can propagate in the phases.

The local equilibrium solidification takes place when the time $\tau_D^i=D_i/(V_D^i)^2$ of the local diffusion relaxation of the chemical composition is essentially less than the characteristic solidification time $\tau_S=D_i/V^2$, where $V=(\mathbf{n}\cdot\mathbf{V})$ is the normal velocity of the liquid-solid interface; $\mathbf{n}$ is the normal interface vector pointed towards the melt; $\mathbf{V}$ is the vector of the solidification front velocity, and $(\cdot)$ is the scalar product of vectors. In this case, the time of relaxation becomes infinitesimal $\tau_D^i\to 0$ and Eqs. (2.1) and (2.3) describe Fick's diffusion transfer in the local equilibrium limits. Thus the transition to the classical Fick law occurs as $\tau_D^i\to 0$, $V_D^i\to\infty$, i.e., when the diffusive speed $V_D^i$ is maximum in comparison with the liquid-solid interface velocity $V$.

When the solidification front moves with a higher velocity, $V\sim V_D^i$, local equilibrium, strictly speaking, does not occur and the mass flux does not depend on the instant value of the chemical composition gradient but is determined by the local prehistory of the mass transfer in the solidifying alloy [see Refs. [13–15] and Eq. (2.1)]. The case $0<V<V_D^i$ corresponds to intermediate regimes of the alloy solidification from a metastable liquid phase to a stable solid one when there may be derivations of concentrations from their local equilibrium values described by a Boltzmann-type distribution. It should be noted that $V_D^i$ limits only the speed of concentrational perturbations, but the normal velocity $V=(\mathbf{n}\cdot\mathbf{V})$ of the liquid-solid interface can be greater than $V_D^i$.

The simple numerical estimates of quenching from the liquid state have shown [15] that the solidification velocity $V$ may be close to the speed $V_D^L$ of the diffusive speed even at cooling rates of $10^4$–$10^5$ K/s and local-nonequilibrium effects appear in a solidifying alloy.

Recently we have discussed the coupled transfer processes which have different space-time scales in a nonlocal medium [4,13,15]. For the nonisothermal rapid solidification of undercooled alloys we can give the following estimates. When the thermal conductivity of the alloy is determined by the phonon oscillation in the solid phase, molecular (ionic) diffusion in a liquid or electron transfer, then thermal relaxation in the alloy takes place at a speed $V_T\sim 10^3$–$10^6$ m/s. Using typical values of the diffusion coefficient $D_i=10^{-10}$–$10^{-11}$ m$^2$/s and a relaxation time $\tau_D^i=10^{-10}$–$10^{-11}$ s (see, for example, [8]) for the diffusive speed $V_D^i$, we have $V_D^i=(D_i/\tau_D^i)^{1/2}=0.1$–$10$ m/s. In any case, the ratio $V_D^i/V_T$ is low: $V_D^i/V_T\sim 10^{-2}$–$10^{-5}$. It follows from this that the local equilibrium in the thermal field of alloys establishes much faster than the local equilibrium of the diffusion field. In this connection, we may describe the heat transfer in both phases as it is governed by the classical local equilibrium heat conduction equation with heat source

$$\varkappa_i\frac{\partial T_i}{\partial t}=\nabla\cdot(\lambda_i\nabla T_i)+Q\mathbf{V}\delta(\mathbf{r}-\mathbf{R}), \tag{2.4}$$

where $\delta(\mathbf{r}-\mathbf{R})$ is the Dirac delta function which depends on the radius vector $\mathbf{r}$ of a point in alloy and the radius vector $\mathbf{R}$ of the interface position; $T$ is the temperature; $\varkappa$ and $\lambda$ are the heat capacity and thermal conductivity, respectively; $Q$ is the latent heat of solidification.

To derive the interface conditions, we integrate Eqs. (2.2) and (2.4) over an infinitesimal zone that includes the liquid-solid interface. The interface conditions are

$$\mathbf{n}\cdot(\lambda_i\nabla T_i)|_S^L+(\mathbf{n}\cdot\mathbf{V})Q=0,\quad T_L=T_S, \tag{2.5}$$

$$\mathbf{n}\cdot(\mathbf{J}_i-\mathbf{V}C_i)|_S^L=0. \tag{2.6}$$

After differentiating Eq. (2.6) by $t$, we have

$$\tau_D^i\left(\frac{\partial \mathbf{J}_i}{\partial t}-C_i\frac{\partial \mathbf{V}}{\partial t}-\mathbf{V}\frac{\partial C_i}{\partial t}\right)\cdot\mathbf{n}|_S^L=0. \tag{2.7}$$

Then, subtracting Eqs. (2.6) and (2.7) and combining the result with Eq. (2.1) we obtain

$$\left[D_i\nabla C_i+\left(\mathbf{V}+\tau_D^i\frac{\partial \mathbf{V}}{\partial t}\right)C_i+\tau_D^i\mathbf{V}\frac{\partial C_i}{\partial t}\right]\cdot\mathbf{n}|_S^L=0. \tag{2.8}$$

Note that the relaxation effects lead to the fact that condition (2.8) includes not only the interface velocity $V$, but also the interface acceleration $\partial\mathbf{V}/\partial t$ [17].

The connection between the interface temperature $T_I=T_L=T_S$ and the concentration $C_L$ is given as [1–4]

$$T_I=T_A-m(V)C_L-V/\beta_0-\Gamma K, \tag{2.9}$$

$$C_S = k(V) C_L , \tag{2.10}$$

where $T_A$ is the temperature of solidification of the alloy main component; $V$ is the normal interface velocity in the vector **n** direction; $\Gamma$ is a capillarity constant which equals $T_A \gamma / Q$; $\gamma$ is the surface tension of the liquid-solid interface; $K$ is the mean curvature of the liquid-solid interface; $\beta_0$ is the kinetic coefficient of interface motion; $m$ is the tangent of the nonequilibrium liquidus line slope which depends on the interface velocity; $k$ is the nonequilibrium partition coefficient which also depends on the interface velocity and defines the solute trapping.

Thus Eqs. (2.3) and (2.4) of heat-mass transfer with interface conditions (2.5), (2.8)–(2.10), and the functions $k$, $K$, $m$ describe the problem of rapid solidification under local-nonequilibrium conditions.

### III. THE STEADY-STATE REGIME

Now let us obtain a steady-state solution of the set of Eqs. (2.3) and (2.4). We view the solidification from a reference frame attached to a solidification front moving at a constant velocity $V$ in the $\xi = x - Vt$ direction. Here we neglect the temperature dependence of the diffusion coefficient in both the liquid ($i = L$) and the solid ($i = S$). In this version, Eqs. (2.3) and (2.4) of heat and mass transfer have the form

$$\frac{d^2 T_i}{d\xi^2} + \frac{V}{a_i} \frac{dT_i}{d\xi} + \frac{QV}{\lambda_i} \delta(\xi) = 0, \tag{3.1}$$

$$D_i [1 - V^2/(V_D^i)^2] \frac{d^2 C_i}{d\xi^2} + V \frac{dC_i}{d\xi} = 0, \tag{3.2}$$

where $a_i = \lambda_i / \varkappa_i$ is the thermal diffusivity. We can get the conditions on the solidification front ($\xi = 0$) from boundary conditions (2.5) and (2.8). They are

$$\lambda_S \frac{dT_S}{d\xi} - \lambda_L \frac{dT_L}{d\xi} = QV, \tag{3.3}$$

$$VC_L + D_L [1 - V^2/(V_D^L)^2] \frac{dC_L}{d\xi} = VC_S + D_S [1 - V^2/(V_D^S)^2] \frac{dC_S}{d\xi}. \tag{3.4}$$

The boundary conditions far from the solidification front are

$$T_L(\infty) = T_0, \quad C_L(\infty) = C_0, \quad \left. \frac{dC_S}{d\xi} \right|_{\xi \to -\infty} = 0. \tag{3.5}$$

The solutions of Eqs. (3.1) and (3.2) which satisfy conditions (3.3), (3.4), and (3.5) are *the solid phase* ($\xi \leqslant 0$)

$$T_S(\xi) = T_I , \quad C_S(\xi) = C_0 , \tag{3.6}$$

and *the liquid phase* ($\xi > 0$)

$$T_L(\xi) = T_0 + (T_I - T_0) \exp\left( - \frac{\xi V}{a_L} \right), \tag{3.7a}$$

$$C_L(\xi) = \begin{cases} C_0 + (C_I - C_0) \exp\left( - \dfrac{\xi V}{D_L [1 - V^2/(V_D^L)^2]} \right), & V < V_D^L \\ C_0 , & V \geqslant V_D^L \end{cases} \tag{3.7b}$$

where $a_L$ is the thermal diffusivity in the liquid and $C_I$ is a concentration of the liquid at the solidification front.

Solutions (3.6) and (3.7a) for temperature have the usual steady-state profiles in both phases [21] except for the value of $T_I$. However, concentration distribution (3.7b) differs substantially from those predicted by the classical parabolic diffusion equation. As it has been shown [15] and following solution (3.7b), when the solidification front motion approaches the diffusive speed, $V \to V_D^L$, the concentration in the liquid reaches the initial concentration of an alloy, i.e., $C_L \to C_0$ for any $0 < \xi < \infty$. Moreover, there is no solute diffusion in the liquid and the solidification process cannot be controlled by the solute redistribution ahead of the solidification front at $V \geqslant V_D^L$ [see Eq. (3.7b) and Ref. [17] ]. This result is in good agreement with the recent experiments [22,23], which observe almost partitionless (diffusionless) solidification if undercoolings exceed a critical undercooling.

Following the standard method of definition of the diffusion layer $\delta_D$ ahead of the solidification front (see Ref. [1], p. 189), an expression for $\delta_D^*$ in a local nonequilibrium situation can be obtained. From (3.7b) we can get

$$\delta_D^* = \begin{cases} 2D_L [1 - V^2/(V_D^L)^2]/V, & V < V_D^L \\ 0, & V \geqslant V_D^L . \end{cases} \tag{3.8}$$

As follows from Eq. (3.8), when the velocity $V$ increases, the solute layer $\delta_D^*$ ahead of the front shrinks more rapidly than expected from the classical mass transport theory (see Fig. 1) in which $\delta_D = 2D_L/V > 0$ for any values $V/V_D^L$.

The behavior of the solute concentration (3.7b) allows us to introduce the effective diffusion coefficient $D^*$ as [17]

$$D^* = \begin{cases} D_L [1 - V^2/(V_D^L)^2], & V < V_D^L \\ 0, & V \geqslant V_D^L . \end{cases} \tag{3.9}$$

If $V \ll V_D^L$, the effective diffusion coefficient $D^*$ reduces to the diffusion coefficient $D_L$ for the local equilibrium condi-

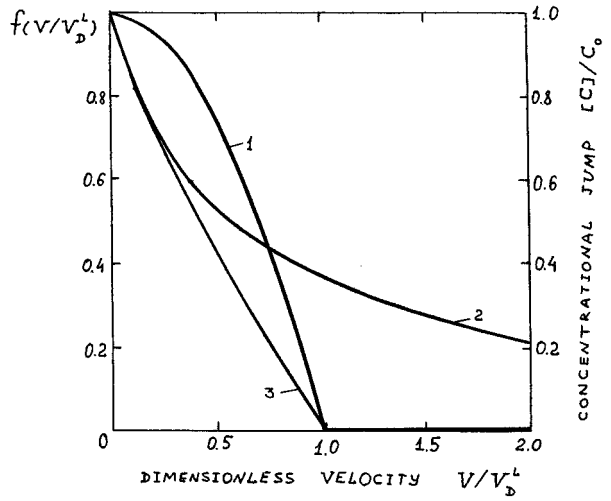


FIG. 1. Curve 1 is the dependence of the dimensionless diffusion layer $\delta_D^*/\delta_D$ and diffusion coefficient $D^*/D_L$ as a function $f(V/V_D^L)=\delta_D^*/\delta_D=D^*/D_L=1-V^2/(V_D^L)^2$ on the dimensionless velocity $V/V_D^L$. Curves 2 and 3 indicate the concentrational jump $[C]/C_0=(1-k)/k$ on the solidification front, where the interface partition coefficient $k$ was used from Aziz's model [12] (curve 2) and present equation (3.12) (curve 3). $k_e=0.5$.

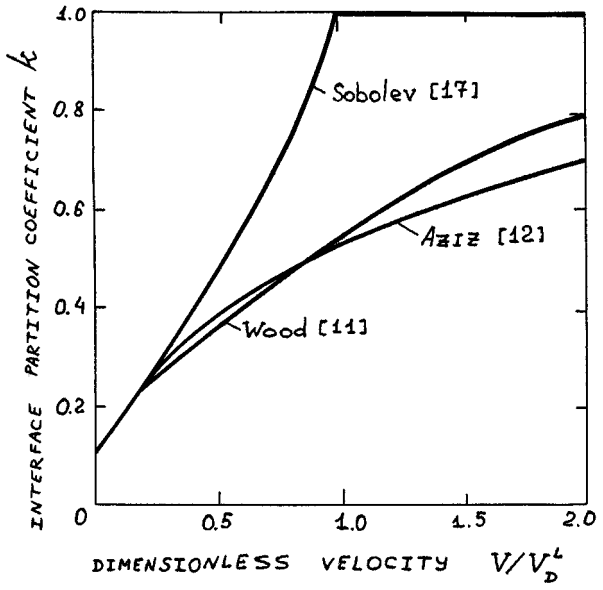


FIG. 2. Curves showing the dependence of the interface partition coefficient $k$ on the dimensionless velocity $V/V_D^L$ according to the models of various investigators ($k_e=0.1$).

tions. But when $V$ is of the order of $V_D^L$, there is an essential difference between $D_L$ and $D^*$. The ratio $D^*/D_L$ is decreased by the parabolic law as $1-V^2/(V_D^L)^2$ in the velocity region $0<V<V_D^L$ and equals zero at $V\geqslant V_D^L$ (see Fig. 1).

The effective diffusion coefficient (3.9) includes the local nonequilibrium effects and can be used to modify some results of the local nonequilibrium theory. For example, the use of $D^*$ in the form of Eq. (3.9) leads to the generalized partition coefficient [17]

$$k=\begin{cases}\dfrac{k_e[1-V^2/(V_D^L)^2]+V/V_D^L}{1-V^2/(V_D^L)^2+V/V_D^L}, & V<V_D^L\\ 1, & V\geqslant V_D^L\end{cases} \tag{3.10}$$

where $k_e$ is the value of the equilibrium partition coefficient at $V\ll V_D^L$.

The known models by Jackson, Gilmer, and Leamy [10], Wood [11], Aziz [12], and expression (3.10) predict the transition to an equilibrium partitioning, $k=k_e$, at a low solidification front velocity, $V\ll V_D^L$, where the models coincide. The transition to complete solute trapping, $k=1$, in the above mentioned models [10–12] occurs only at infinite interface velocity, $V\to\infty$. However, expression (3.10) clearly demonstrates that the transition to complete solute trapping, $k=1$, occurs at $V=V_D^L$ (see Fig. 2).

Now let us consider the concentration profiles in more detail. Using expression (3.10), we rewrite solutions (3.6) and (3.7b) in the form

$$C_S(\xi\leqslant 0)=C_0 \quad \text{for any } V, \tag{3.11a}$$

$$C_L(\xi>0)=\begin{cases}C_0\left[1+\dfrac{(1-k_e)[1-V^2/(V_D^L)^2]}{k_e[1-V^2/(V_D^L)^2]+V/V_D^L}\exp\left(-\dfrac{\xi V}{D_L[1-V^2/(V_D^L)^2]}\right)\right], & V<V_D^L\\ C_0, & V\geqslant V_D^L.\end{cases} \tag{3.11b}$$

In the limits $V/V_D^L\to 0$, the solution (3.11b) reduces to the local equilibrium solution obtained by Ivantsov [24] and Tiller *et al.* [25]. As the ratio $V/V_D^L$ increases, the solute concentration $C_L(0)$ at the interface will decrease. When $V\geqslant V_D^L$, the concentration in both phases has the initial composition of an alloy $C_S(\xi)=C_L(\xi)=C_0$ (Fig. 3). Note that this result differs fundamentally from the classical local-equilibrium case where $C_L(\xi)\to C_0$ only when $V\to\infty$ (see, for example, Ref. [26]).

In the local nonequilibrium approach, solution (3.11), Eq. (3.10) and condition (2.10) give an expression for the concentration jump $[C]\equiv C_L(0)-C_S(0)$ at the front. The jump is

$$[C]=\begin{cases}\dfrac{C_0(1-k_e)[1-V^2/(V_D^L)^2]}{k_e[1-V^2/(V_D^L)^2]+V/V_D^L}, & V<V_D^L\\ 0, & V\geqslant V_D^L.\end{cases} \tag{3.12}$$

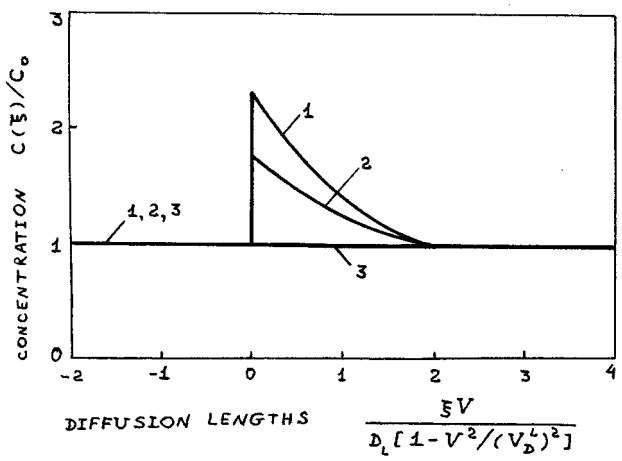


FIG. 3. The solute profiles computed for different values of the dimensionless velocity $V/V_D^L$: 1—$V/V_D^L=0.001$; 2—$V/V_D^L=0.5$; 3—$V/V_D^L\geqslant 1$. $k_e=0.5$. Distance $\xi$ has been nondimensionalized with respect to diffusion length, $D_L[1-V^2/(V_D^L)^2]/V$.

As expression (3.12) predicts, an alloy has equal concentrations, $C_L(0)=C_S(0)$, on the solidification front at $V\geqslant V_D^L$ (see Fig. 1). This means that the lines of nonequilibrium liquidus and solidus will coincide on the kinetic phase diagram at the finite velocities $V\geqslant V_D^L$ of the solidification of an alloy.

## IV. UNDERCOOLING DISTRIBUTION IN THE LIQUID PHASE

Now let us examine the undercooling $\Delta T$ in the bulk liquid and at the solidification front, where $\Delta T$ is a difference between the temperature $T_{\rm liq}$ of liquid on the kinetic diagram of alloy state and the true temperature $T_L$ in the temperature field. Then we have the relation

$$\Delta T(\xi\geqslant 0)=T_{\rm liq}(\xi)-T_L(\xi), \tag{4.1}$$

where

$$T_{\rm liq}(\xi)=T_A-mC_L(\xi) \tag{4.2}$$

is the equation of the nonequilibrium liquidus line on the kinetic phase diagram.

Substituting Eqs. (2.9), (2.10), (3.7a), (3.7b), and (4.2) for Eq. (4.1), for the case of the flat solidification front (the mean curvature of the solid-liquid interface is zero, i.e., $K=0$) we obtain the expression

$$\Delta T(\xi\geqslant 0)=\Delta T_0\left[1-\exp\left(-\frac{\xi V}{a_L}\right)\right]+\Delta T_C\left[\exp\left(-\frac{\xi V}{a_L}\right)-\exp\left(-\frac{\xi V}{D_L[1-V^2/(V_D^L)^2]}\right)\right]+(\Delta T_K+\Delta T_N)\exp\left(-\frac{\xi V}{a_L}\right),\quad V<V_D^L, \tag{4.3a}$$

$$\Delta T(\xi\geqslant 0)=\Delta T_0-(\Delta T_0-\Delta T_K-\Delta T_N)\exp\left(-\frac{\xi V}{a_L}\right),\quad V\geqslant V_D^L. \tag{4.3b}$$

Here

$$\Delta T_0=T_A-m_0C_0-T_0 \tag{4.4}$$

is the initial (base) undercooling in the liquid phase far from the solidification front, $m_0$ is the tangent of the equilibrium liquidus line slope,

$$\Delta T_C\equiv m[C]=\begin{cases} mC_0(1-k)/k, & V<V_D^L \\ 0, & V\geqslant V_D^L \end{cases} \tag{4.5}$$

is the preexponential factor of the constitutional undercooling [see the second term in the right side of Eq. (4.3a)] caused by the solute redistribution in the liquid phase ahead of the solidification front, $\Delta T_C$ has a meaning of the nonequilibrium temperature interval of solidification on the kinetic phase diagram of the alloy,

$$\Delta T_K=V/(\beta V_D^L) \tag{4.6}$$

is the kinetic undercooling on the solidification front, $\beta=\beta_0/V_D^L$ is the ratio of the kinetic coefficient $\beta_0$ and the diffusional speed $V_D^L$, and

$$\Delta T_N=(m-m_0)C_0 \tag{4.7}$$

is the undercooling defined by the difference between the equilibrium liquidus temperature $T_A-m_0C_0$ and the nonequilibrium liquidus temperature $T_A-mC_0$ on the kinetic phase diagram.

As follows from Eq. (4.3), the liquid is undercooled on the solidification front ($\xi=0$) and far from it ($\xi\to\infty$):

$$\Delta T=\begin{cases} \Delta T_K+\Delta T_N, & \xi=0 \\ \Delta T_0, & \xi\to\infty. \end{cases} \tag{4.8}$$

Condition (4.8) is different from the classical solution of the constitutional undercooling problem [24,25,27] in which the liquid is undercooled, but the solidification front and infinite point in liquid are in equilibrium ($\Delta T_0=\Delta T_K=\Delta T_N=0$). In the local-equilibrium approximation, $V\ll V_L$, and under the conditions $T_0=T_A-mC_0$, $m\to m_0$ the general solution (4.3a) reduces to the known Borisov expression [27] which was obtained on the basis of Ivantsov's solution [24] (a discussion about this local-equilibrium expression is also given in Ref. [4], p. 107).

Solutions (3.6) and (3.7a), consistently with the temperature balance (3.3), give the temperature $T_I$ on the solidification front,

$$T_I=T_Q+T_0, \tag{4.9}$$

where $T_Q=Q/\varkappa_L$ is the temperature of adiabatic solidification. Having equated the two expressions (2.9) and (4.9), the

initial undercooling $\Delta T_0$ on the flat solidification front ($K=0$) can be divided into the next parts,

$$\Delta T_0 \equiv T_A - m_0 C_0 - T_0 = \begin{cases} \Delta T_T + \Delta T_K + \Delta T_C + \Delta T_N, & V < V_D^L \\ \Delta T_T + \Delta T_K + \Delta T_N, & V \geq V_D^L \end{cases} \quad (4.10)$$

where $\Delta T_T = T_Q$ is the purely thermal undercooling. We can conclude that as it follows from Eqs. (4.5)–(4.7) and (4.10), the constant velocity of the solidification front is possible (nonzero kinetics of the attachment of atoms at the solidification front, $V>0$) if

$$\Delta T_0 > \Delta T_T + \Delta T_C + \Delta T_N = T_Q + mC_0(1-k)/k + (m-m_0)C_0, \quad V < V_D^L$$
$$\Delta T_0 > \Delta T_T + \Delta T_N = T_Q + (m-m_0)C_0, \quad V \geq V_D^L. \quad (4.11)$$

Under these conditions the solidification front can move in the steady-state regime.

Figure 4 shows kinetic phase diagrams in the coordinates' ''temperature-chemical composition'' in the steady-state regime of local nonequilibrium solidification of a dilute alloy. In connection with Eqs. (4.4)–(4.10), the ratio between the contributions of the undercoolings $\Delta T_T, \Delta T_K, \Delta T_C, \Delta T_N$ to the total undercooling $\Delta T_0$ at $V<V_D^L$ is shown [see Fig. 4(a)]. It is evident that in this case the interval of solidification is shorter than in the equilibrium situation, $\Delta T_C = mC_0(1-k)/k < \Delta T_C^0 = m_0 C_0(1-k_e)/k_e$. This demonstrates a tendency to formation of more homogeneous alloys as the solidification velocity $V$ increases in the range $0<V<V_D^L$. Then, with finite solidification velocities, $V \geq V_D^L$, the confluence of nonequilibrium lines of liquidus and solidus occurs [see Fig. 4(b)]. In this case the solidification of the alloy proceeds without changing its chemical composition, $C_L(0)=C_S(0)=C_0$, at the front and with a constant slope $m^*$ of the nonequilibrium line of solidification, Fig. 4(b). As follows from Eq. (3.7b), at $V \geq V_D^L$ the concentration in the liquid phase is also equal to the initial one, $C_L(\xi)=C_0$. Hence the solidification of the alloy will proceed completely partitionless with the initial chemical composition. This conclusion is in agreement with the results in [28], where on the basis of molecular dynamics computer simulation techniques it has been shown that the complete solute trapping occurs when the liquid-solid interface velocity attained its critical steady-state value.

Our treatment of the undercoolings lends strong support to the idea that the diffusive speed $V_D^L$ is one of the most decisive parameters in rapid solidification processes. As we showed, the distribution of the undercooling $\Delta T(\xi \geq 0)$ and the initial undercooling $\Delta T_0$ have the constitutional undercooling only at $V<V_D^L$ [see Eqs. (4.3.1) and (4.10)]. When $V \geq V_D^L$, the constitutional undercooling is zero [see Eqs. (4.5) and (4.10)]. In the latter case, i.e., when the homogeneity of the solute distribution in the liquid phase occurs, $C_L(\xi>0)=C_0$, the flat solidification front will be absolutely stable relative to the constitutional undercooling because of its lacking.

Thus if the front velocity $V$ is higher than the diffusive speed $V_D^L$ the distribution of undercooling in the liquid is due to the initial undercooling $\Delta T_0$ and the kinetic terms such as $\Delta T_K$ and $\Delta T_N$. As follows from Eq. (4.3), at the critical point $V=V_D^L$ a transition from a diffusion-limited to a purely thermally and kinetically controlled growth occurs. Such a transition has been observed in experiments on rapid solidification of undercooled alloys [2,5,7,8,23,29,30]. This result has a clear physical meaning. A source of concentrational perturbations, i.e., liquid-solid interface, moving at a velocity equal to or higher than the maximum speed of these perturbations cannot disturb the alloy ahead of itself. Therefore when the interface velocity $V$ passes through the critical point $V=V_D^L$ the solidification mechanism changes qualitatively, and the undercooling in liquid will not depend on the solute diffusive profile.

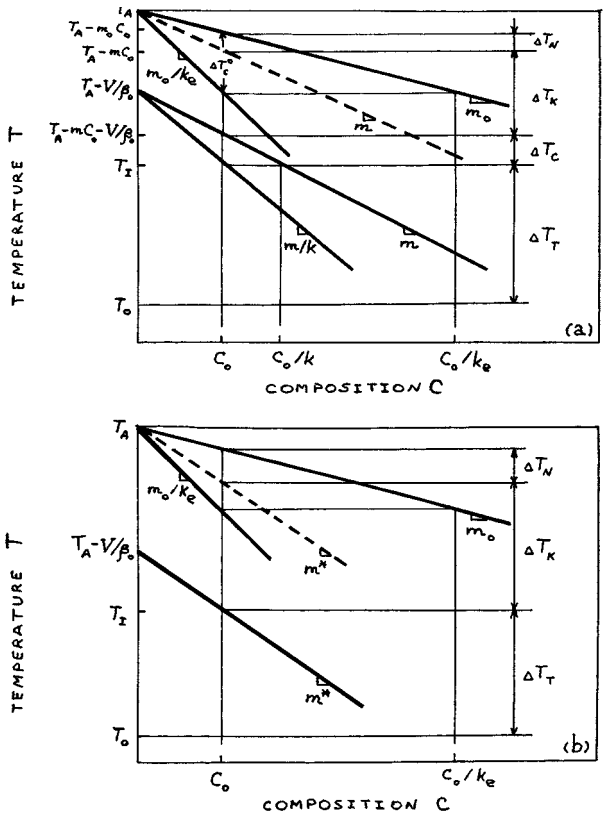


FIG. 4. Determination of different contributions ($\Delta T_N, \Delta T_K, \Delta T_C, \Delta T_T$) into the total undercooling $\Delta T_0$ on a part of the kinetic phase diagram of a dilute alloy. Equilibrium diagram of phase state defined by the lines of the liquidus and solidus which have the slopes $m_0$ and $m_0/k_e$, respectively. Dotted line represents the line that connects the melting point $T_A$ of the main alloy component with the interface composition in the liquid in the absence of the interface attachment kinetic effect. Nonequilibrium liquidus and solidus lines in the presence of the interface attachment kinetic effect have the slopes $m(V)$ and $m(V)/k(V)$, respectively. (a) Effect of local nonequilibrium on composition in the liquid phase for given velocity $0<V<V_D^L$ at the solidification front and in the solute diffusion field. The composition of solid is $C_0$ under the steady-state regime and at the self-consistent temperature $T_I$ at the solidification front, $T_I = T_0 + T_Q = T_A - mC_0/k - V/\beta_0$. (b) Confluence of the nonequilibrium liquidus and solidus lines into one line with the slope $m^*$ at $V \geq V_D^L$. Temperature interval $\Delta T_C$ of nonequilibrium solidification is zero. Value of the kinetic undercooling $\Delta T_K$ increases as the velocity $V$ increases.

## V. DISCUSSION

Now let us consider undercooling on the front and in the liquid under local nonequilibrium conditions in more detail.

For the numerical estimates, we decided to take a Ag-Cu dilute alloy which is often used in the rapid solidification processes. In our calculations we choose the next physical constants: $k_e=0.44$, $m_0=6.46$ K/wt %, $D_L=2.1\times10^{-5}$ cm$^2$/s, $T_A=1233.5$ K, $T_Q=337$ K, $\beta_0=10$ (cm/s)/K [9,31,32]. Here we give the estimate of the diffusive velocity as $V_D^L=D_L/l_0=170$ cm/s, where $l_0$ is a length scale related to the interatomic distance equal to $1.235\times10^{-7}$ cm. We shall calculate undercoolings in a Ag–1 wt % Cu alloy at the initial temperature of $T_0=850$ K.

For the total definition of undercoolings, we shall use an expression for the nonequilibrium liquidus line slope $m$ dependent on the partition coefficient $k$ [1,2]. This yields

$$m=m_0\left\{1+\frac{1}{1-k_e}\{k_e-k[1-\ln(k/k_e)]\}\right\}. \qquad (5.1)$$

The insertion of Eq. (3.10) into Eq. (5.1) for the generalized partition coefficient $k$ gives direct dependence $m$ on the ratio $V/V_D^L$.

The distribution of undercoolings in the liquid phase and at the solidification front is defined by the set of equations (4.3)–(4.10) and (5.1) with inequalities (4.11). The results of calculation of the undercooling $\Delta T(\xi)$ in liquid are plotted in Fig. 5. The undercoolings $\Delta T_C$, $\Delta T_K$, and $\Delta T_N$ at the solidification front are plotted versus the ratio $V/V_L$ in Fig. 6.

The undercooling $\Delta T(\xi)$ has a smooth profile on the heat lengths, $a_L/V$, which do not depend on the variation of the ratio $V/V_D^L$ [see Fig. 5(a)]. In the meantime, the distribution of undercooling $\Delta T(\xi)$ on the diffusion lengths, $D_L[1-V^2/(V_D^L)^2]/V$, is changed from the local equilibrium smooth profile [$V\ll V_D^L$, see curve 1 in Fig. 5(b)] to the constant value only due to the kinetic undercooling on the front, $\xi=0$ [$V\geq V_D^L$, curve 3 in Fig. 5(b)]. This change occurs at an almost zero value of the kinetic sum $\Delta T_K+\Delta T_N$ on the solidification front (at $V\ll V_D^L$) up to the zero value of the constitutional undercooling in liquid (at $V\geq V_D^L$) (see Fig. 6). In this case the nonequilibrium interval of solidification, $\Delta T_C$, degenerates into zero, and the alloy composition corresponds to a point on the line with a constant slope $m^*=(m_0\ln k_e)/(k_e-1)$ [see Eq. (5.1) at $k=1$] on the kinetic diagram of solidification, Fig. 4(b).

Notwithstanding the fact that at $V<V_D^L$ the value of the undercooling $\Delta T(\xi)$ at any point $\xi$ near the front is not higher than 3% of the initial undercooling $\Delta T_0$ (see Figs. 5 and 6), it is the inhomogeneity of the distribution $\Delta T(\xi)$ that leads to the instability of the flat front of solidification [3,33,34]. In this situation, growing structures—cells and dendrites—will be formed inside the diffusional layer [1,2,4,8]. However, this diffusional layer degenerates in the limits $V\to V_D^L$ [see Eq. (3.8)], and in the velocity range $V\geq V_D^L$ the constant undercooling will occur on the diffusion lengths [see curve 3 in Fig. 5(b)]. In the latter case, i.e., at $V\geq V_D^L$, the profile of undercooling $\Delta T(\xi)$ manifests only on the heat lengths [see Fig. 5(a)]. Thus a transition from diffusionlike growing structures to thermal-like ones can occur. A quite similar change in behavior of Ni-B dendrites has been shown in the experiment by Eckler *et al.* [23]. This transition has been observed experimentally by Walder and Ryder [30] on a rapid crystal growth from undercooled Ag-Cu melts.

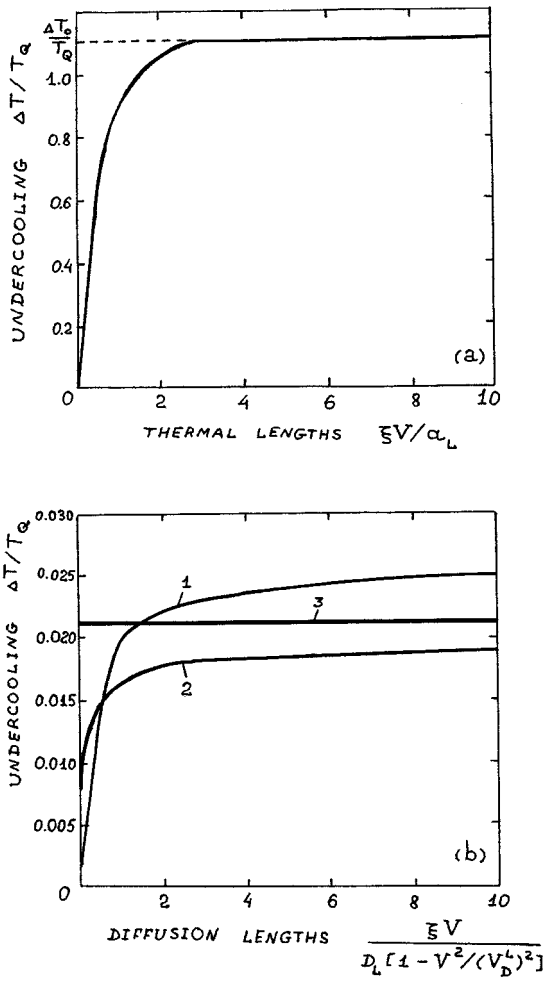


FIG. 5. The undercooling $\Delta T(\xi)$ distribution in the liquid phase of Ag–1 wt % Cu alloy on the thermal (a) and diffusion (b) lengths. Distance $\xi$ has been nondimensionalized with respect to thermal length, $a_L/V$, and diffusion length, $D_L[1-V^2/(V_D^L)^2]/V$.

Possible transition to thermal growing structures in alloys is directly connected with the solute partitioning process and the beginning of the partitionless solidification. As we qualitatively showed in Fig. 2, local-nonequilibrium effects significantly influence the solute partitioning. For quantitative demonstration of this influence we can use the results of Kittl *et al.*'s experimental measurements [35] on Si-As dilute alloy solidification. In Fig. 7 the partition coefficient $k$ is shown as a function of the solidification velocity $V$. In comparison with the experiment [35] we correlate two models, one of which takes into account both the finite speed of substance propagation in the bulk liquid and the deviation from equilibrium at the solidification front [present investigation, Eq. (3.10)], and the other model takes into account the deviation from equilibrium at the solidification front only [12]. Evidently, if the two extreme points marked in Fig. 7 near the value $V=2$ m/s are interpreted within the limits of experimental error as a complete partitionless solidification result, one can see that Eq. (3.10) gives quite a satisfactory result in comparison with the experiment. It should be noted that there is a considerable uncertainty in the choice of the

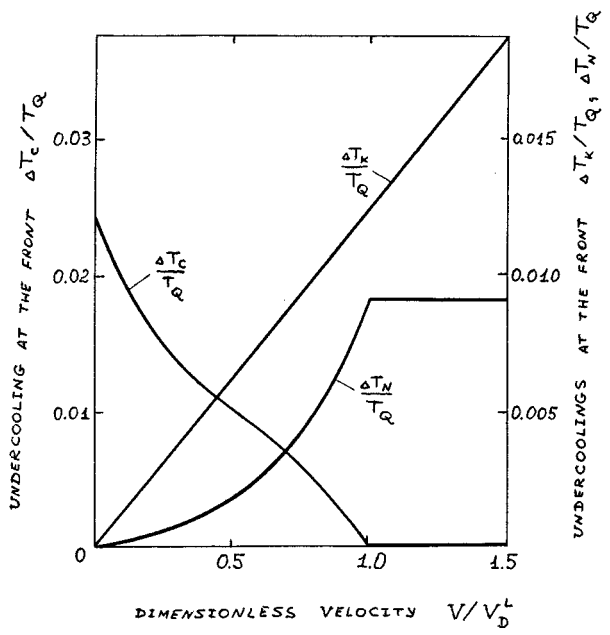


FIG. 6. The undercoolings at the flat solidification front of Ag–1 wt % Cu alloy versus the dimensionless velocity $V/V_D^L$.

value of the diffusive speed $V_D^L$. For example, in Ref. [31] the range of the value of the diffusive speed is evaluated within the limits of one order ($V_D^L = 0.4–4.0$ m/s for Ag-Cu dilute alloys). In the works [35,36] when interpreting the experiments on Si-As alloy solidification, various models were used where the values of the diffusive speed were different from one another more than 12 times, $V_D^L = 0.035–0.46$ m/s. For a satisfactory comparison with the experiment (Fig. 7) we used a value of the diffusive speed $V_D^L = 1.2$ m/s. Therefore in our opinion, for further quantitative correlations between the theory and experiment, a more detailed investigation of the solute partitioning process is necessary. Particularly, it is necessary to obtain experimentally the rates of solidification under which the transition to complete solute trapping and partitionless solidification occurs. Also, it is necessary to make more exact the notion of the diffusive speed $V_D^L$. In the present investigation we assumed that the diffusive speed at the solidification front equals the diffusive speed in the bulk liquid. This assumption may lead to discrepancy between the predictions of the theory and the experiment if for an alloy the diffusion coefficient and interatomic distance have essentially different values at the solidification front and inside the bulk liquid.

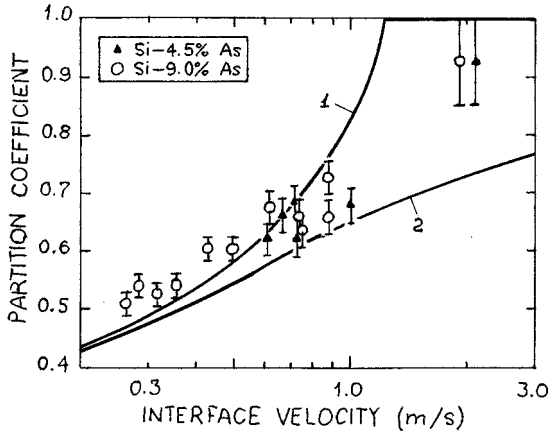


FIG. 7. Quantitative comparison ''solidification velocity–solute partitioning function'' for the present investigation, Eq. (3.10) (curve 1), and the dilute continuous growth model [12] (curve 2) with the experimental data [35] (symbols ○ and ▲). $k_e = 0.35$, $V_D^L = 1.2$ m/s.

It is also pertinent to note the remarkable experiments on revealing chemical homogeneity of dendritic alloys. Miroshnichenko points out [7] the fact that in the splat cooling process for the binary Al-Mg, Al-Mn, Cu-Sn, and Cu-Sb systems cooled at a rate above $10^6$ K/s the concentration in the core of dendrites equals the initial chemical composition of alloys. In all alloys the concentration changed discontinuously at a cooling rate equal to $10^6$ K/s. At the same cooling rate the partition coefficient $k$ which was defined as the ratio between the solute concentration in the solid and in the liquid at the interface changed sharply from the near equilibrium value $k_e$ up to $k=1$ (a brief discussion about Miroshnichenko's experiment is given by Chernov in Ref. [8], p. 196). The partition coefficient $k=1$ occurs at higher rates [7].

It is evident that the analytical treatment of the function ''undercooling–dendritic growth velocity'' at high cooling rates [6,7] and from deeply undercooled alloy melts [23,29] can be made, if, according to the model developed in the work, one takes into account the deviation from local equilibrium at the liquid-solid interface and inside the bulk liquid. Unfortunately, this analytical calculation is difficult to carry out at present as the existing functions defining the crystal growth shape (for example, one of these functions is a so-called ''Ivantsov function,'' see Refs. [1,4,37]) are based on the local equilibrium approximation. This makes it difficult to describe the experiment adequately [38], and the definition of the nonequilibrium crystal growth shape can become further development of the local-nonequilibrium model of alloy solidification.

It has also been shown in experiments [6] under cooling rates $5\times10^6$ K/s that in the melts of aluminum-magnum alloys the eutectic decomposition is suppressed. The supersaturated solid solutions with the initial liquid chemical composition of the alloy are formed. The sharp change in the crystallization mechanism proves that the cooling rate increasing above the critical value leads to qualitative changes in kinetic and mass transport processes.

Thus the morphological transitions in growth forms and a change of solidification regimes occur at high undercoolings. As it has been estimated by Herlach [2], the change of the growth regimes is connected with the attainment of the critical growth velocity which is equal to the atomic diffusive speed.

All our theoretical results lend strong support to the idea that the diffusive speed $V_D^L$ is one of the most decisive parameters which phenomenologically represents the effect of local nonequilibrium in the rapid solidification processes. When $V \geqslant V_D^L$, solution (3.11b) implies that the solute concentration ahead of the solidification front is undisturbed and reaches the initial concentration of the alloy. The correct definition of the solute layer $\delta_D^*$ and the effective diffusion coefficient $D^*$ also demonstrate the absence of the diffusion

processes at $V \geqslant V_D^L$ [see Eqs. (3.8), (3.9)]. This result is in agreement with the physical meaning that a source of perturbation, i.e., the liquid-solid interface, moving at a velocity higher than the maximum speed of perturbations cannot disturb the medium ahead of itself. Thus when the interface velocity $V$ passes through the critical point $V = V_D^L$, the undercooling depends only on the temperature profile in the liquid and kinetic undercooling at the interface [see Eq. (4.3b)], but it does not depend on the solute diffusive profile. At this point, a transition from diffusion-limited to purely thermally controlled growth can occur.

The role which the diffusive speed plays in rapid solidification processes can be favorably compared with the anisotropy effect or the growth kinetics of a liquid-solid interface. Like the achievement by the front of the diffusive speed, well-known effects such as the change of crystallographic directions of growing crystals [39] or exchange of the atomic kinetics mechanism [40] offer breaks on the curves $V$ versus $\Delta T$ at some critical undercooling $\Delta T^*$. It seems plausible that the nonmonotonous dependence $V$ versus $\Delta T$ observed in experiments on deep undercooled alloy solidification [5,22,23,29] is governed by the set of listed causes. Therefore the detailed experimental study for elucidation of the causes of the nonmonotonous dependence $V$ versus $\Delta T$ will require a special consideration of the theoretical approach.

## VI. CONCLUSIONS

(i) Local nonequilibrium solidification of a binary alloy has been investigated analytically in the steady-state regime of isotropic liquid-solid interface motion. Our model takes into account the relaxation to local equilibrium of the solute flux in both phases and incorporates the diffusive speed as the most important parameter governing the solute concentration field. This approach leads to the non-Fickian diffusion problem in rapid solidification described by a hyperbolic-type partial differential equation.

(ii) The most significant changes in the solidification regimes under local-nonequilibrium conditions occur near the critical point $V = V_D^L$, i.e., when the solidification velocity $V$ equals the diffusive speed $V_D^L$ in the liquid phase. At $V \geqslant V_D^L$ an alloy solidifies completely partitionless with the initial chemical composition.

(iii) The shift from the local equilibrium in the diffusion field and solute distribution at $V < V_D^L$ contribute significantly to the total undercooling defined as the sum of thermal, kinetic, and caused by the solute distribution constitutional undercooling. At $V \geqslant V_D^L$ there is no influence of the diffusion field, and the undercooling in the liquid will be defined only by thermal undercooling in the liquid and kinetic undercooling at the growth front. Thus at $V \geqslant V_D^L$ the constitutional undercooling is absent and the flat solidification front will be absolutely stable relative to the constitutional undercooling. The transition from a diffusion-limited to a purely thermally and kinetically controlled solidification regime occurs.


[1] W. Kurz and D. J. Fisher, *Fundamentals of Solidification*, 3rd ed. (Trans Tech, Aedermannsdorf, Switzerland, 1992).

[2] D. M. Herlach, Mater. Sci. Eng. **R12**, 177 (1994).

[3] W. J. Boettinger, S. R. Coriell, and R. F. Sekerka, Mater. Sci. Eng. **65**, 27 (1984).

[4] P. K. Galenko and V. A. Zhuravlev, *Physics of Dendrites* (World Scientific, Singapore, 1994).

[5] R. Willnecker, D. M. Herlach, and B. Feuerbacher, Phys. Rev. Lett. **62**, 2709 (1989); Appl. Phys. Lett. **56**, 324 (1990).

[6] I. S. Miroshnichenko and I. M. Galushko, in *Crystallization Kinetics and Mechanism*, edited by N. N. Sirota (Nauka i Tekhnika, Minsk, 1973), p. 356 (in Russian).

[7] I. S. Miroshnichenko, *Quenching from the Liquid State* (Metallurgia, Moscow, 1982) (in Russian).

[8] A. A. Chernov, in *Modern Crystallography*, edited by M. Cardona, P. Fulde, and H.-J. Queisser, Springer Series in Solid-State Science Vol. 36 (Springer, Berlin, 1984), Vol. III.

[9] W. J. Boettinger, R. J. Schaefer, F. S. Biancaniello, and D. Shechtman, Metall. Trans. A **15**, 55 (1984).

[10] K. A. Jackson, G. H. Gilmer, and H. J. Leamy, in *Laser and Electron Beam Processing of Materials*, edited by C. W. White and P. S. Peercy (Academic, New York, 1980), p. 104.

[11] R. F. Wood, Appl. Phys. Lett. **37**, 302 (1980).

[12] M. J. Aziz, J. Appl. Phys. **53**, 1158 (1982); P. M. Smith and M. J. Aziz, Acta Metall. Mater. **42**, 3515 (1994).

[13] S. L. Sobolev, Usp. Fiz. Nauk **161**, 5 (1991) [Sov. Phys. Usp. **34**, 101 (1991)].

[14] S. L. Sobolev, Phys. Lett. A **163**, 101 (1992).

[15] P. K. Galenko, Kristallografya **38(6)**, 238 (1993) [Crystallogr. Rep. **38**, 836 (1993)]; Phys. Lett. A **190**, 292 (1994).

[16] S. L. Sobolev, Phys. Lett. A **197**, 243 (1995).

[17] S. L. Sobolev, Phys. Lett. A **199**, 383 (1995).

[18] D. Jou, J. Casas-Vazquez, and G. Lebon, Rep. Prog. Phys. **51**, 1105 (1988); *Extended Irreversible Thermodynamics* (Springer, Berlin, 1992).

[19] S. L. Sobolev, J. Phys. (France) III **3**, 2261 (1993); Phys. Rev. E **50**, 3255 (1994).

[20] P. K. Galenko, Dokl. Akad. Nauk **334**, 707 (1994) [Phys. Dokl. **39**, 111 (1994)].

[21] J. Rosental, J. Trans. ASME **68**, 849 (1946).

[22] R. Willnecker, D. M. Herlach, and B. Feuerbacher, Phys. Rev. Lett. **62**, 2709 (1989).

[23] K. Eckler, R. F. Cochrane, D. M. Herlach, B. Feuerbacher, and M. Jurisch, Phys. Rev. B **45**, 5019 (1992).

[24] G. P. Ivantsov, Dokl. Akad. Nauk SSSR **81**, 179 (1951).

[25] W. A. Tiller, K. A. Jackson, J. W. Rutter, and B. Chalmers, Acta Metall. **1**, 428 (1953).

[26] A. A. Wheeler, G. B. McFadden, and W. J. Boettinger, Phys. Rev. E **47**, 1893 (1993).

[27] V. T. Borisov, *Theory of Two-Phase Zone of Metal Ingot* (Metallurgia, Moscow, 1987) (in Russian).

[28] S. J. Cook and P. Clancy, J. Chem. Phys. **99**, 2175 (1993).

[29] K. Eckler, D. H. Herlach, and M. J. Aziz, Acta Metall. Mater. **42**, 975 (1994).

[30] S. Walder and P. L. Ryder, J. Appl. Phys. **74**, 6100 (1993); Acta Metall. Mater. **43**, 4007 (1995).

[31] W. Kurz, B. Giovaniola, and R. Trivedi, Acta Metall. **34**, 823 (1986).

[32] D. A. Huntley and S. H. Davis, Acta Metall. Mater. **41**, 2025 (1993).

[33] W. W. Mullins and R. F. Sekerka, J. Appl. Phys. **34**, 323 (1963); **35**, 444 (1964).

[34] G. J. Merchant and S. H. Davis, Acta Metall. Mater. **38**, 2683 (1990).

[35] J. A. Kittl, M. J. Aziz, D. P. Brunco, and M. O. Thompson, J. Cryst. Growth **148**, 172 (1995).

[36] J. A. Kittl, M. J. Aziz, D. P. Brunco, and M. O. Thompson, Appl. Phys. Lett. **64**, 2359 (1994).

[37] G. P. Ivantsov, Dokl. Akad. Nauk SSSR **58**, 576 (1947).

[38] In Ref. [37] Ivantsov assumed that the crystal growth shape must be an isoconcentrational interface which grows under quasiequilibrium conditions. When the crystals grow under nonequilibrium conditions, and the shift from local equilibrium at the interface and in the diffusion field of bulk phases is manifested, the crystal shape must be different from Ivantsov's solution [37]. In contrast with the calculations which used the Ivantsov function (see Refs. [23, 29]), our unpublished results of a computer simulation based on the system of equations (2.3)–(2.5), (2.8)–(2.10), and (3.10) show that a full scenario of solute and thermal dendrites in all regions of undercoolings can be obtained. Also, we suppose that in rapid solidification the effect of growth anisotropy can influence the function ''undercooling–dendrite growth velocity'' considerably [see M. Ben Amar, Phys. Rev. A **41**, 2080 (1990); K. Eckler and D. M. Herlach, Mater. Sci. Eng. A **178**, 159 (1994)].

[39] S. K. Chan, H. H. Reimer, and M. Kahlweit, J. Cryst. Growth **32**, 303 (1976); E. Ben-Jacob, Contemp. Phys. **34**, 247 (1993).

[40] G. A. Alfintsev and D. E. Ovsiyenko, in *Growth of Crystals*, edited by E. I. Givargizov (Nauka, Moscow, 1980), p. 121 (in Russian); E. S. Kucherenko, Izv. Akad. Nauk SSSR Met. **N3**, 116 (1978); D. E. Ovsiyenko, *Nucleation and Growth of Crystals from Melts* (Naukova Dumka, Kiev, 1994) (in Russian).